Renewable Energy 231 (2024) 120869

Contents lists available at ScienceDirect

Renewable Energy

journal homepage: www.elsevier.com/locate/renene

Geometry optimization of a floating platform with an integrated system of wave energy converters using a genetic algorithm

Chisom Ekweoba [a,*], Dan El Montoya [b], Lander Galera [b], Susana Costa [b], Sarah Thomas [b], Andrej Savin [a], Irina Temiz [a]

[a] Department of Electrical Engineering, Uppsala University Box 65, 75103 Uppsala, Sweden
[b] Floating Power Plant A/S, Park Alle 382, Vallensbæk, 2625, Denmark

ARTICLE INFO

Keywords:
Wave energy converter
Floating platform
Geometry optimization
Extended degree of freedom
Genetic algorithm

ABSTRACT

This study uses a genetic algorithm(GA) to investigate the practicality of optimizing the geometry and dimensions of a floating platform, which houses pitching wave energy converters (WEC). Using frequency-domain analysis, sensitivity tests for the search start point, choice of optimized variable, number of iterations, simulation time, and contents of the search space are made. Results show that the required number of iterations to convergence increases with an increased number of optimized variables. Furthermore, for the studied platform geometry, no single global optimum exists. Instead, various combinations of characteristic features can lead to comparable performances of the integrated wave absorber. Finally, it is observed that when the solution space is controlled and made to contain a subset of potential solutions known to improve the system performance, computation time, absorption efficiency and range are observed to improve. Additionally, the GA optimum tends towards platform geometries for which the wave absorber's resonance response corresponds to the dominating wave climate frequencies. A key contribution of this study is the controlled manipulation of the solution space to contain a subset of potential solutions that enhance system performance. This controlled approach leads to improvements in computation time, absorption efficiency, and range of the system.

1. Introduction

Wave energy converters (WECs) are devices used to convert the energy in waves into other forms of energy for useful applications, for example, electricity generation, water desalination, etc. Whatever the application may be, the basic objective of WECs is to find an efficient means of converting this energy from one form to another. The application of WECs to electricity generation dates back several decades [1] and has since gained more popularity. The effective conversion of wave energy into electricity relies on the efficiency of a series of energy conversion stages, spanning from the waves themselves to the wave absorber, followed by the power take-off system and transmission. Consequently, research focused on enhancing WEC absorption efficiency holds significant relevance.

Several studies have used geometry and dimension optimization to improve WEC hydrodynamic coefficients and WEC absorption efficiency. In [2], the shape of the bottom part of a cylindrical WEC is used to increase the motion response while accounting for the effect of viscous damping. In a similar study, the shape optimization of a point absorber, which translates along a straight-sloped path that is defined by the inclination of some guiding rods [3], was done using the brute-force approach. The authors adopted an exhaustive search method with a heuristic approach, and the optimum geometry obtained is able to harvest twice as much wave energy as the original design.

The optimization of a wave absorber (WA) often goes hand in hand with the optimization of other device parameters, such as the power take-off (PTO) damping and, in some cases, the submerged volume, which serves as a metric for estimating the cost. For instance, in [4,5], different geometries of point absorbers, and the PTO damping coefficients were compared for power maximization and resonance response, respectively. Similarly, in the frequency-domain analysis study done by [6] the objective of the optimization was to ascertain the buoy dimensions that can optimize its heaving velocity and a corresponding PTO damping coefficient while [7] including the wave absorption bandwidth as an objective function.

While the studies mentioned above have shown that optimizing the geometry and dimensions of WECs can enhance overall system performance, these investigations have typically focused on a limited number of geometries. As a result, the parametric sweep and brute force

* Corresponding author.
E-mail address: chisom.ekweoba@angstrom.uu.se (C. Ekweoba).

https://doi.org/10.1016/j.renene.2024.120869
Received 3 July 2023; Received in revised form 13 March 2024; Accepted 22 June 2024
Available online 26 June 2024

approach were employed. These methods become computationally expensive with an increased number of candidate solutions. Depending on the size of the solution space that needs to be searched in order to obtain the most efficient geometry, different optimization methods are adopted. A commonly used method for finding wave absorber optimal geometry, among other optimization parameters, is based on a genetic algorithm (GA). In this method, several candidate solutions are tested against an objective function or a set of objective functions in a sequence of pseudo-random searches. This meta-heuristic search method has found its application in wave energy converter optimization, where a large number of possible solutions are tested. In the studies presented in [8,9], GA is used to optimize the collector shape of a WEC. In [10], a differential evolution algorithm-based optimization studies the relationship between the submerged volume of a buoy and the power production performance of the isolated WEC. Validating against parameter sweep, results show that the ratio of computational time of using the differential evolution algorithm to parameter sweep is 1 : 35.

A review done in [11] categorizes a set of geometry optimization studies of WEC based on the WEC type, geometry type, objective function, and optimization procedure. However, most of these studies have focused on enhancing the wave-structure interaction of the WEC devices, and not much work has been done to account for interactions between two or more structures in designs where there are multi-bodies and relative motions between bodies resulting in extended degrees of freedom (DoF) motion.

Additional modes of motion for the wave absorbers relative to the platform, developed internally by the Floating Power Plant (FPP), are employed to accurately model the interaction between the wave absorbers and the floating platform. The specific methods used for these additional modes of motion will not be detailed in this study. However, the approach is influenced by the method described in [12] for modelling the motion of deformable floating bodies. Similar applications can be found in [13], where a wave energy device with air-filled compressible submerged volumes is analysed, and in [14], which presents a wave-activated device utilizing relative pitch motions between two modules to compress and expand a hydraulic cylinder. These examples demonstrate the use of extended Degrees of Freedom (DoF) motion to define the relative motion of floaters or modules within wave energy systems.

In this study, a Genetic Algorithm (GA) is employed to optimize the geometries of a floating wind turbine platform that incorporates four pitching wave absorbers, as depicted in Fig. 1. The wave absorber itself is shown in Fig. 2. The surrounding parts of the platform, which house the wave absorbers, are referred to as the chamber.

The use of GA in engineering design applications, particularly in structural designs, has been well-established [15–17].

In our study, we refine the GA methodology to tailor the characteristic features of a floating platform, with the goal of optimizing its interaction with pitching wave absorbers while adhering to constraints. Our objective is to investigate the feasibility of this approach and develop strategies to enhance its effectiveness. The optimization parameters include various platform characteristic features, contributing to a vast solution space. However, the exponential growth in the number of candidate geometries, resulting from the increased number of variables, makes finding the optimum configuration computationally expensive. Our method addresses this challenge by carefully controlling the search space quality, enabling the discovery of favourable solutions while reducing computation time. This approach represents an advancement of the GA method specifically tailored for optimizing floating platforms, with broader applicability to multi-variable optimization problems.

The rest of the paper is organized as follows: Section 2 presents the mathematical model of the wave-structure interaction and the wave data used for this study. In Section 3, the formulation of the optimization algorithm is presented, and validations of the methods are shown in Section 4. Results for the analysis performed, discussion and conclusions are presented in Sections 5–7, respectively.

Fig. 1. The floating power plant device.
Source: Reproduced with permission from ([18]).

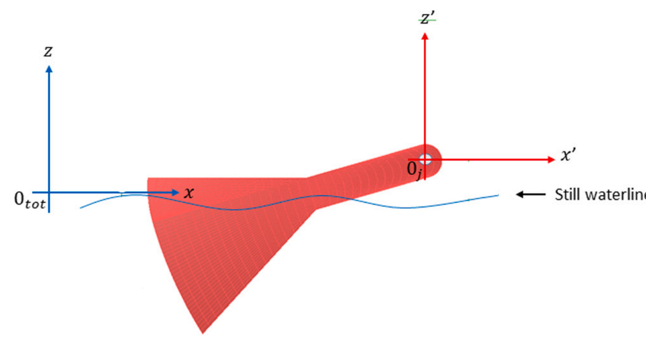

Fig. 2. Absorber geometry showing the absorber coordinate system with the origin at 0_j and the total body coordinate system with the origin at 0_{tot}; modelled using a low-order analytical method and visualized with Multisurf CAD software.

2. Mathematical model

2.1. Equation of motion

The equation of motion of the floating body is derived from Newton's second law of motion:

$$\mathbf{M}\ddot{\Theta} = \vec{F}_e + \vec{F}_r + \vec{F}_h + \vec{F}_o \tag{1}$$

where $\mathbf{M}$ is the mass matrix of the structure, $\ddot{\Theta}$ is its acceleration, and $\vec{F}_e, \vec{F}_r, \vec{F}_h$ are the excitation force, radiation force, and hydrostatic restoring force respectively. $\vec{F}_o$ represents other external forces such as the mooring, drag and power take-off (pto) forces. Due to linearity, excitation force is represented as the sum of the forces from the incident and scattered waves; $\vec{F}_{FK}$, $\vec{F}_{sc}$. When small amplitude motion is assumed, the hydrostatic restoring force, F_h, is linearly proportional to the displacement of the floating body. It is, therefore, expressed as $\vec{F}_h = \mathbf{C}\xi$, where ξ is the body displacement and $\mathbf{C} = \mathbf{C}_{hyd} + \mathbf{C}_{grav}$ is the hydrostatic restoring coefficient matrix comprising of the buoyancy and gravitational restoring coefficient matrices, $\mathbf{C}_{hyd}$ and $\mathbf{C}_{grav}$ respectively. The radiation force is divided into two parts, one of which is linearly proportional to the floating body velocity, referred to as its radiation damping $\mathbf{B}$, and the other which is linearly proportional to its acceleration, known as the added mass $\mathbf{A}$.

Assuming that the system is completely linear, has reached its steady state, and including power take-off ($\mathbf{B}_{pto}$), linearized quadratic drag ($\mathbf{B}_{drag}$) and simplified linearized mooring system ($\mathbf{C}_{mooring}$), Eq. (1)

Hm0[m] \ Te[s]	5.39	7.18	8.98	10.78	12.57	14.37	16.17	17.96
0.5	0.00053	0.00076	0.00040	0.00000	0.00000	0.00000	0.00000	0.00000
1.5	0.11583	0.12826	0.06884	0.02441	0.00606	0.00066	0.00004	0.00000
2.5	0.05658	0.22997	0.13005	0.06135	0.01779	0.00239	0.00024	0.00000
3.5	0.00003	0.02882	0.04474	0.03245	0.01517	0.00324	0.00051	0.00003
4.5	0.00000	0.00056	0.00545	0.00535	0.00563	0.00217	0.00026	0.00000
5.5	0.00000	0.00000	0.00047	0.00091	0.00100	0.00088	0.00007	0.00000
6.5	0.00000	0.00000	0.00000	0.00006	0.00002	0.00008	0.00002	0.00000
7.5	0.00000	0.00000	0.00000	0.00000	0.00000	0.00000	0.00000	0.00000

Fig. 3. Scatter diagram showing sea states' occurrence frequency taken from PLOCAN.

can be rearranged and rewritten to derive the transfer function, $H(\omega)$, of the displacement of a floating body as a function of wave angular frequency, ω:

$$\mathbf{H}(\omega) = \frac{\Theta}{A} = \frac{\vec{F}_{FK} + \vec{F}_{sc}}{-\omega^2(\mathbf{A}+\mathbf{M}) + j\omega(\mathbf{B}+\mathbf{B}_{pto}+\mathbf{B}_{drag}) + (\mathbf{C}_{hyd}+\mathbf{C}_{grav}+\mathbf{C}_{mooring})} \tag{2}$$

where A is the wave amplitude and $j = \sqrt{-1}$. In this study, the hydrodynamic and hydrostatic coefficients $\mathbf{A}$, $\mathbf{B}$, $\mathbf{C}_{hyd}$ and forces, $\vec{F}_{FK}$, $\vec{F}_{sc}$ are calculated using a programme which is based on linear potential flow theory, WAMIT.

2.2. Wave conditions

The performance of the WEC is studied when it is operating in irregular waves. The irregular waves are represented in this case as summations of sinusoidal waves with different amplitudes, frequencies, lengths and phases. A wave spectrum is used to describe an irregular wave. Fig. 3 shows the wave climate of the test site, PLOCAN,[1] in Spain used in this study.

For this study, the JONSWAP spectrum is used to define the waves mathematically and is expressed as [19]

$$S_{ij}(\omega) = \bar{\alpha} g^2 \omega^{-5} e^{(-\beta_0(\omega/\omega_p)^{-4})} \gamma^a. \tag{3}$$

where i and j are indices for the significant wave height, H_s and energy period, T_e, respectively. γ is the peakedness parameter and has a value of 3.3, and ω_p is the frequency at which the spectrum has its peak amplitude. β_0 is the shape factor and equals 1.25. g is the gravitational acceleration, while a and $\bar{\alpha}$ are modified Phillips constants which are defined as

$$a = e^{-((\omega-\omega_p)^2/(2\sigma^2\omega_p^2))} \tag{4}$$

and

$$\alpha = 5/16(H_s/\omega_p^2)^2(1 - 0.287\log\gamma). \tag{5}$$

where T_p is the period corresponding to the peak amplitude of the spectrum. T_p is related to the energy period, T_e by [20,21];

$$T_p = T_e/C, \tag{6}$$

where C is a coefficient between T_p and T_e and is taken as $C = 0.87$.

3. Methodology

For this study, the platform with absorbers system is modelled in the frequency domain using wave analysis software, WAMIT. The software uses the user-defined geometry, along with details of its mass properties and external forces (when applicable), to analyse the wave-structure interaction and generate the frequency-dependent hydrodynamic coefficients. The definition of the submerged geometry can be done using different methods. One option is the use of CAD software, such as Multisurf, which can be integrated directly into WAMIT. Another option is to explicitly specify the coordinates of the vertices of individual panels that make up the submerged body. In order to optimize the platform geometry using GA, several calls will be made to WAMIT for each new geometry to obtain the system's response for that unique solution. This necessitates the use of a geometry model that can easily be modified and integrated into the software. In order to save the computational cost of remodelling the system numerically for each modified set of variable combinations, an analytical model of the system is created to enable fast geometry changes while maintaining its orientation and preserving features that do not need to change. The analytical model is created by writing a customized subroutine for individual panels on the chamber and wave absorber into the WAMIT geomxact.f file. The subroutine is then called directly from the WAMIT geometry data file, where the desired dimensions are specified. Each patch is defined using an input parametric coordinate u, v whose domain must lie within $[-1, 1]$, in the analytical representation and the outputs are Cartesian coordinates x, y, z of the boundaries of each patch with respect to a body-fixed coordinate system. The patches' coordinates are made interdependent to allow flexibility for when the geometries are modified. More details on how to link the user-defined subroutine to the rest of the WAMIT executable code can be found in [22].

The wave absorbers' annual energy production and absorption frequency range are considered yardsticks for estimating the approximate wave absorber efficiency and are used as the objective functions. For comparability, the geometry and mass properties of the wave absorbers integrated into the platform remain unchanged throughout the study. The impact of the wave absorber geometry is not included here, and will be done in future studies. The wave absorbers are coupled to the platform, and they all move as a single unit with six degrees of freedom. In addition to these modes, the hinged wave absorbers also pitch relative to the platform; therefore, the wave absorbers' extended DoF motion is taken into account in this study. Additional modes of motion for the wave absorbers relative to the platform, developed internally by the Floating Power Plant (FPP), are employed to accurately model the interaction between the wave absorbers and the floating platform. The specific methods used for these additional modes of motion will not be detailed in this study. However, the approach is influenced by the method described in [12] for modelling the motion of deformable floating bodies. Similar applications can be found in [13], where a wave energy device with air-filled compressible submerged volumes is analysed, and in [14], which presents a wave-activated device utilizing relative pitch motions between two modules to compress and expand a hydraulic cylinder. These examples demonstrate the use of extended Degrees of Freedom (DoF) motion to define the relative motion of floaters or modules within wave energy systems.

The linear formulation of the system's hydrodynamics is experimentally validated, as detailed in the study by [23]. Additionally, the method employed to optimize the operation of the wave absorbers is outlined in [24], which is also applied in the current study. The

[1] https://plocan.eu/.

mass distribution of the platform, analysed using the beam elements method, is confirmed in [25]. Consequently, for each tested geometry, the overall system dynamics are accurately captured.

3.1. Mass properties

Modifying the geometry of the floating platform results in a change in its mass, position of its centre of gravity, and radii of gyration. These parameters impact the system response and, consequently, the WEC's power absorption. In using the GA optimization method, the process needs to consider the role that these parameters play for every possible geometry in the search space. The mass distribution of the platform and wave absorbers are generated separately and then combined to obtain the total body mass distribution. Before searching for the optimum platform geometry, it is important to ensure that the wave absorbers are already operating at their optimum. This is done using an extensive analytical search for the absorbers' optimal ballast configuration, as detailed in [24]. This ballast search entails calculating the absorber response amplitude operator, RAO, for a range of possible ballast mass-center of gravity (COG) location combinations within the wave absorber, from which the combination that provides the desired resonance frequency is selected. This method takes into account the ballast compartment sizing, the impact of the choice of ballast matter, the position of the pivot point of the pitching wave absorber and its tilting (rest) angle about the hinge. The optimal ballast mass, m_b, and centre of gravity, $\vec{r}_{g,b}$, are then combined with the pre-known empty wave absorber mass, m_a, and centre of gravity, $\vec{r}_{g,a}$. For the platform, a beam model of the floating platform developed by FPP is used. The mass property is approximated from the beam model. The model is a representation of individual components of the platform by beams with corresponding lengths, masses and occupying the same positions in the platform coordinate system (PCS). The mass distribution of the entire platform is then computed from the contribution of each beam. In other words, all components of the platform are represented as interlinked and interdependent beams with predetermined mass per unit length per beam.

3.2. Optimization method

In this study, a multi-variable-objective optimization problem is solved to find the optimum platform geometry. For this purpose, the genetic algorithm is used. Fig. 4 shows a flow chart of the algorithm. This is a search technique that is based on the principle of genetics and natural selection and is chosen because of its ability to search a large solution space [26]. Also, unlike some other methods, it does not require finding the derivative of the objective function. Due to the stochastic nature of the genetic algorithms, repeatability is almost infeasible. Even if the search space contains just one possible optimum solution, the likelihood that the multiple runs will start at the same point and follow the same route to the solution is almost zero. Therefore, repeated runs are recommended to get the most desirable results.

The objective function and set of constraints

The purpose of this study is to find the geometry of the floating platform for which the integrated wave absorbers have a wide absorption frequency range and maximize the annual energy production (AEP) for a range of sea states. Constraints are implemented to ensure the stability and practicality of the solution, preventing unrealistic or impractical geometry configurations as well as configurations that are not stable and might result in large displacements. The mean power absorbed by the wave absorbers in an irregular sea state, as in Fig. 3, is computed from the combination of absorbed power in regular waves, which are defined through specific wave height and period combinations. $\vec{P}(\omega_k, \beta)$, as, [27],

$$\vec{P}_{ij} = \sum_{k=1}^{N} \frac{\vec{P}(\omega_k, \beta)}{\epsilon_a^2} A_{ij,k}^2, i = 1, 2, 3 \dots m, j = 1, 2, 3 \dots n, \quad (7)$$

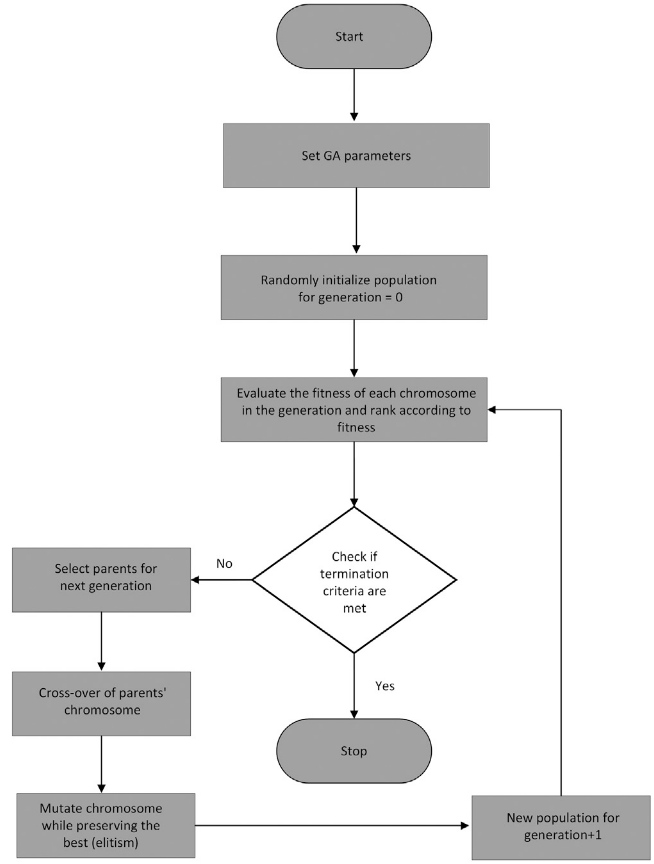

Fig. 4. The genetic algorithm process flow chart.

where $\vec{P}_{ij}$ is the mean power absorbed in irregular waves for a given sea state that has amplitude A_{ij}, while $i = 1, \dots, m$ and $j = 1, \dots, n$ are the significant wave height and peak period components, respectively, of the spectrum divided into N equidistant frequency or period steps. A_{ij} is defined as;

$$A_{ij} = (2S_{ij}\Delta\omega)^{0.5}, \quad (8)$$

where $\Delta\omega$ is the step size of the frequency and S_{ij} is as defined in (3). $\vec{P}_k = \vec{P}(\omega_k, \beta) = 0.5B_{pto}^{ij}\omega_k^2|\Theta(\omega_k)|^2$ is the mean absorbed power in regular waves as a function of regular wave frequency, ω_k, evaluated for each wave heading, β, for a regular wave amplitude of ϵ_a. B_{pto} is the PTO damping coefficient and Θ is the WA angular displacement. Here the wave heading, β, is assumed constant at 180° in the wave absorber coordinate system and the wave amplitude in regular wave $\epsilon_a = 1$, therefore (7) can be simplified as:

$$\vec{P}_{ij} = \sum_{k=1}^{N} \vec{P}_k(\omega_k) A_{ij,k}^2, \quad (9)$$

The annual energy production, as derived from Eq. (7), becomes:

$$AEP = \sum_{i=1}^{m} \sum_{j=1}^{n} \vec{P}_{ij} E_{ij}, \quad (10)$$

where E_{ij} is the probability of a certain significant wave height, H_s and peak period, T_p, combination occurring in a year. For the system under study, we observed that for some system geometries the RAO spikes at some wave periods and maintains relatively low values at other periods. Since more interest lies in geometries where RAO maintains relatively high values within our desired bandwidth of wave periods, the mean RAO for a given bandwidth is used as a weighting factor, W, for the objective function. The Fitness/objective Factor (FF) is calculated as the product of W (weighting factor) and AEP (Annual Energy Production). This value is normalized based on the original geometry's FF, resulting in a relative improvement factor. The objective function, FF, is, therefore:

$$FF = W \cdot AEP, \tag{11}$$

where $W = \frac{\sum_{p=1}^{P} RAO_p}{P}, p = 5, 5.1, 5.2, 5.3, \dots, 25$, p are wave periods between 5 s and 25 s while P is the number of wave periods between 5 s and 25 s. Some constraints are put in place to ensure that the system search converges but not to an unstable solution. The coordinates of the platform are constrained to ensure that the surfaces of the platform and wave absorber maintain a safe distance and do not intersect at any point, as this will produce unrealistic results. Additionally, considering that the floating platform also serves as the foundation for a wind turbine, some constraints are set to ensure that the solution is able to support the wind turbine adequately; the static heel and static trim are estimated as the angular displacement of the system about the x and y axis respectively, in the total body coordinate system as in Fig. 2. The angular displacement is calculated as:

$$DF_{x,y} = \frac{180(C_{hdy} + C_{grav})F_{x,y}}{\pi}, \tag{12}$$

where $DF_{x,y}$ is the angular displacement about the x and y axis in degrees, and $F_{x,y}$ is the thrust force on the wind turbine in the x and y directions. For this study, this force is considered constant and independent of various factors, including wind speed, turbine characteristics, and aerodynamic properties. It is the force on the turbine for the predominate sea state and wind speed at the site location. The static heel is equal to DF_x while static trim is equal to DF_y The objective function is set to zero when either the static trim (pitch angle displacement) or static heel (roll angle displacement) is greater than 5°. This is to ensure that the final result does not present an unstable geometry. Therefore, the constrained objective function is given as:

$$FF = \begin{cases} W \cdot AEP, & \text{if static heel or static trim} \leq 5^\circ \\ 0, & \text{otherwise} \end{cases} \tag{13}$$

4. Methods validation

4.1. Sanity check of the optimization algorithm

The algorithm is checked to determine how close it gets to finding an optimum. To do this, a single variable, V1 as in Table 1, for which the global optimum value can easily be determined is used. The acceptable span of the variable is set, and a parametric sweep done through this range is compared to results from the GA search. Out of the GA searches that were done, half were constrained to have the same initial population, and the other half had a randomly selected start-up population. This is done in order to test for repeatability and also to observe the influence of the initial position on the search convergence in both cases. Convergence is observed to be reached after an average of 100 iterations, with a population size of 15 (i.e., the number of unique geometries analysed for each iteration) and a mutation rate of 0.2. Irrespective of the number of iterations, the GA search matches the parameter sweep closely.

From Fig. 5, it is seen that the GA search appears to be in agreement with the parametric sweep.

5. Results

Table 1 shows the definition of the variables chosen for the optimization study. The effect of the optimization of these dimensions is presented in this section.

Table 1
Definition of the variables optimized.

Variable	Description
V1	Distance between the fore pontoon and aft pontoon
V2	Distance between the spoiler top and the still water line
V3	Chamber length
V4	Bottom plate height
V5	Turret extension
V6	Chamber depth
V7	Pontoon foot height
V8	Support foot height
V9	Pontoon pillar length
V10	Support foot length

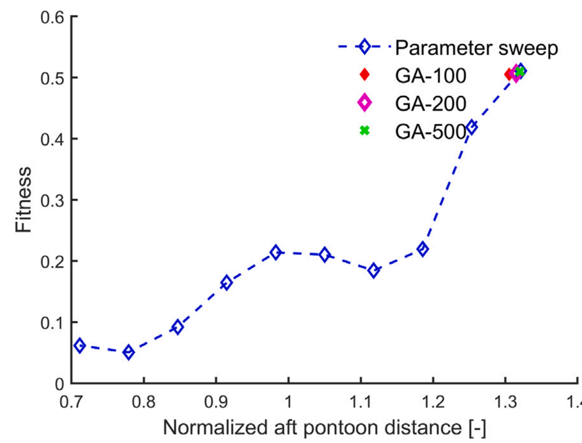

Fig. 5. Single variable optimization using GA at 100, 200, and 500 iterations vs. parametric sweep. The variable dimensions are normalized by the original geometry.

5.1. Individual variable influence

In Fig. 6, a parametric sweep of individual variables is presented. All other variables are kept constant while the values of each optimization variable are varied between predefined ranges, resulting in different fitness values. This is to observe the level of impact each variable has on the fitness, independently and the direction of influence relative to the position of the base geometry. The variation range of each of the variables is within ±30% of the base/original geometry. This is except for V6 and V9, where it is impossible to do so without creating an impractical geometry; in these cases, the upper and lower boundaries, respectively, are set to the values of these variables in the base case geometry. It is observed that some variables have a more significant influence on fitness compared to others, even though individual parametric sweep offers only marginal improvement to fitness. Fig. 6 illustrates the Fitness value range obtained when varying each individual optimization variable independently. This parametric sweep helps identify the potential contribution of each variable to the fitness function.

5.2. Search start point

The starting point of the GA search routine could play a role in whether the local or global optimum is found. The starting point of the GA search routine could influence the optimality of the solution, impacting its proximity to the true global optimum. The sensitivity of the start point is further investigated. Independent GA searches are performed for three different combinations of the variables to be optimized: set 1 comprises of variables (V1–V10), set 2 contains (V1–V2), and set 3 (V1–V5, V10). Each search is done within 50 iterations. In the beginning, each set's search tends to start at approximately the same fitness and gradually makes its way up as the number of iterations

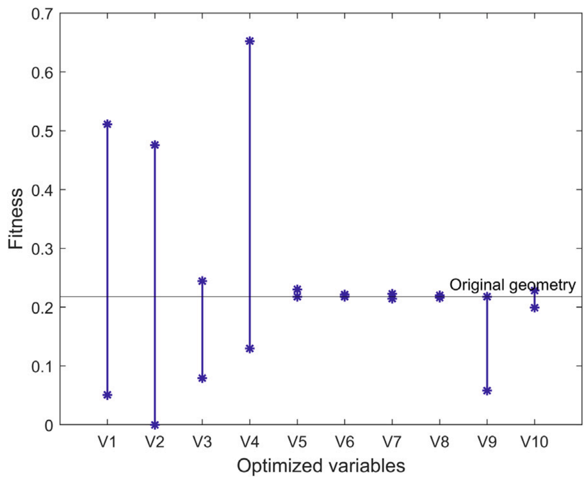

Fig. 6. Fitness function for individual optimization variable showing to what degree each variable impacts the fitness compared to the original geometry.

progresses, as in Fig. 7. However, by starting a search with the best result obtained from a previous search, the tendency to find better solutions with few iterations is increased.

It is, therefore, recommendable to start the search by running a few search iterations. The choice of the number of iterations is left to the discretion of the researcher, as there is no known ideal number. Furthermore, since there is a possibility for the search to get stuck in a local optimum position, this approach could also be valuable if the search is stuck, as seen in Fig. 7(b).

5.3. Computation time and generations to convergence

The amount of time taken to complete an optimization study is known to be dependent on three key factors [11], which include the capabilities of the machine that is used for the computation, the objective function and complexity of the model, and the chosen optimization algorithm and its implementation.

The GA optimization search is utilized in this study to seek the optimal combination of the variables outlined in Table 1. Since the floating platform has a number of characteristic features that could be optimized, a comparison is made to ascertain how the number of optimization variables will influence the number of generations to converge. The number of variables to be optimized is increased sequentially from two to ten.

The GA search is set to terminate if the fitness value is equal to 35 times the value of the original geometry or when the number of iterations gets to 200, whichever comes first. The search starting point is based on the results obtained from "Run 2" in the start point sensitivity test shown by Fig. 7(b). The simulation time for the optimization search is then tested across different computing capacities, 4 core, 6 core, and 16 core processor machines. The 6 and 16 core processor computers have 12 and 32 logical processors, respectively. WAMIT is set to run in parallel and uses all the available cores of the computer. At run-time, the 4 and 6 core machines are observed to utilize 100% of their computing capacities. The 16 core machine, on the other hand, uses approximately 70% of its capacity. From Fig. 8 it is seen that it takes approximately 21 h, per 100 iterations, to complete a run on a 4 core processor machine and approximately half the time when using a 16 core processor computer. The 6 core processor PC takes 12.5 h per 100 iteration.

The averaged time allocation between WAMIT simulation and pre- and post-processing using MATLAB for single geometry analysis is presented in Table 2. The pre-processing computation includes generating WAMIT input files from the set of optimization parameters in

Table 2
Explicit computation time allocation for one geometry analysis using computers with different computing capabilities.

Computer specification	4 core 8 GB RAM	6 core 32 GB RAM	16 core 128 GB RAM
WAMIT simulation [s]	40	21	18
MATLAB pre & post-processing [s]	10	6.2	5

the current generation while the post-processing involves collecting the hydrodynamic and hydrostatic data from WAMIT output files, calculating mass properties from the beam model and then the objective function according to Eq. (13).

Approximately 80% of the computation time goes into the wave-structure interaction simulation using WAMIT, as can be observed from Table 2. Since only the panel sizes change and the number of panels remains unchanged, the effective change in computation time for changing various panel sizes remains negligible, hence, the negligible effect of the number of variables optimized on the overall computation time.

It can be observed from Fig. 8 that with an increased number of variables, the solution space tends to widen, which results in more iterations required for convergence and, consequently, the computation time.

5.4. Solution space

The absorption range, W, and normalized annual energy production, AEP, as in (11), are observed for the different number of variables optimized. Fig. 9 shows the solution space that the GA search spans depending on how many variables are optimized. It is observed that there is an influence of the nature of the impact of individual variables on the solution space. When two variables are optimized, the solution tends towards lower absorption efficiency, with the high absorption occurring at an intermediate absorption range of roughly 0.8. This could be a result of the solution space containing a relatively fewer number of permutations but, at the same time, containing a relatively positive influence of variables. By adding V3 and making the number of variables optimized three, we see a decrease in the predominant value of the distribution to absorption range of approximately 0.5, but with increased absorption efficiency. Moving from 4 variables upwards, higher absorption and spread are observed. This behaviour could be credited to the relatively positive influence of variables 4 included in the search space. However, no outstanding dissimilarities are observed when the number of variables optimized is increased from four to eight. The observation is due to the low influence level of variables V5 to V8, as shown in Fig. 6. With the further widening of the solution space to ten variables, a downward spiral of the number of search results attaining high AEP and range of absorption is seen. A possible reason for this is the addition of variations that could potentially negatively influence the fitness, specifically V9, (as seen in Fig. 6).

In order to investigate how the permutation of the variables and the choice of variables studied at a time affects the absorption range and, consequently, the fitness, the optimization of 6 variables containing the sequentially selected variables is compared to different combination sets of 6 variables. The new set of 6 variables study contained the most influential variables according to Fig. 6, i.e., V1, V2, V3, V4, V9 and V10. This investigates if the most influential variables alone are enough to attain desirable results within a shorter computational time. Due to the knowledge that these influential variables have the potential to cause a negative influence, another set of variables is created. It contains the same influential variables, but with the variation boundaries shifted in an attempt to eliminate their negative influences.

For the set of 6 more influential variables, it is observed from Fig. 10 that performance did not necessarily get better; however, there

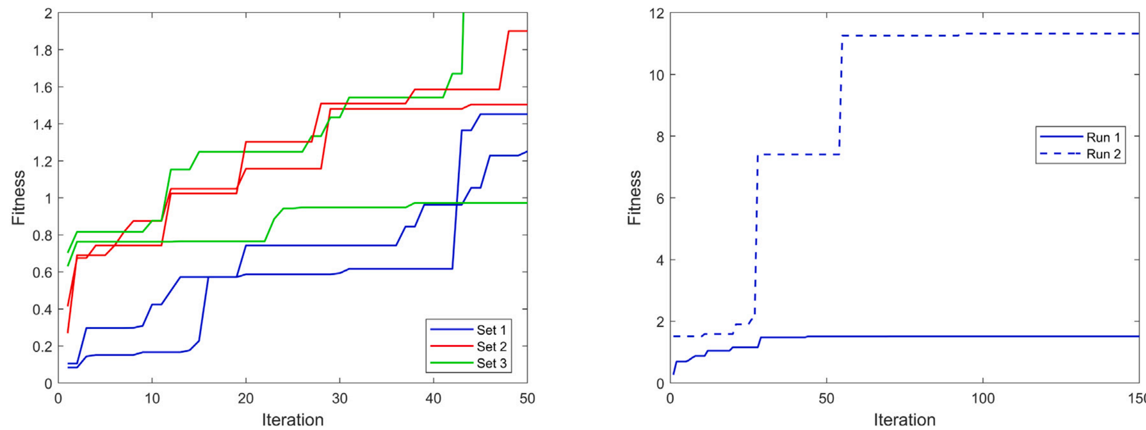

(a) (b)

Fig. 7. (a) Iteration progression vs fitness for 3 unique sets of variables to be optimized: set 1 (V1–V10), set 2 (V1–V2), set 3 (V1–V5, V10). For each set, 2 independent simulations are run. (b) The final geometry result of run 1 is set as the search starting point of run 2 for the set of variables (Set 2 as in (a)).

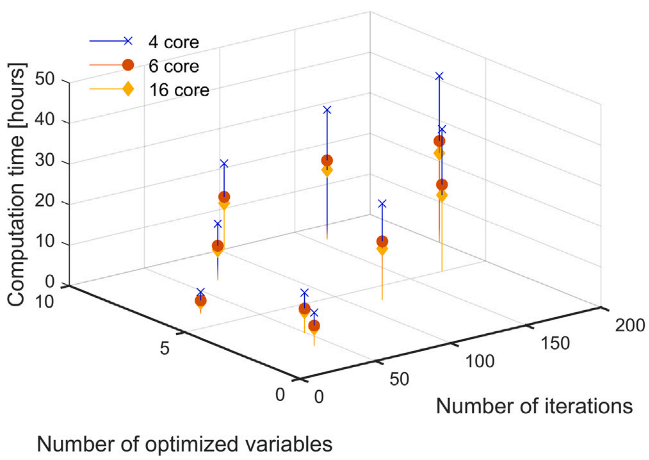

Fig. 8. Computation time for different computing capacities and the number of optimized variables required for convergence at fitness equal to 3.5.

is quick convergence, and the simulation time was half as long when the boundary conditions are streamlined. Curtailment of the search boundaries also appears to give rise to solutions that offer a wider range of absorption. The normalized wave absorber's response amplitude operator (RAO) for the geometry that gives the optimal solution according to the GA search is shown in Fig. 10b. It can be seen that a more desirable response is attained by a reduced peak at high frequency, widening the RAO curve and moving the resonance frequency closer to the predominant sea state.

For a given fitness function, having more streamlined variables' boundaries and opting for variables that impact fitness the most could be an excellent way to speed up computation, improve the likelihood of convergence of the search, and improve overall performance.

5.5. *Absolute optimum check*

Results from the GA searches that give approximately the same fitness function values are compared. This addresses the inquiry regarding the existence of a definitive set of variables that yield the optimal geometry. In other words, is there an absolute optimal for the platform geometry? An attempt to answer this question is made by seeking out the GA searches that resulted in fitness function value within a given narrow range. The variables combination that resulted in these fitness function values are then compared. For this purpose, a set of 6 variable optimization searches are used. The six most positively influential variable, V1, V2, V3, V4, V5, V10, are chosen for this purpose. Fig. 11 shows geometry variation and corresponding fitness function values.

The fitness functions of this set differ from one another by less than 0.03, which is approximately 3% of the baseline, yet only little similarity exists between corresponding variables. It shows the feasibility of attaining approximately the same fitness by different combinations of geometric features. This observation suggests that there may not be a single global optimum for the floating platform's geometry, but several local optima are found.

5.6. *Resonance response*

The motion response of the platform and absorbers are compared for cases where: (1) a combination of features offering best performances according to individual variables' parametric sweep; (2) while considering only the most influential variables, the solution space is curtailed to cancel negative influence; (3) the original geometry that we started with. It is important to note that the original geometry is optimized for a different site, the North Sea, considering both the absorption efficiency and reduction of steel used, while the presented study optimizes absorption at the PLOCAN site.

The relative pitch response amplitude operator (RAO) of the absorber shown in Fig. 12 indicated how the curtailment of the solution space not only improves the amplitude and range of the RAO but also tends to provide geometry whose resonance response corresponds better to the predominant sea-state. When compared to the original geometry and result from the GA search, the result obtained from performing a parameter sweep for individual variables appears to be the least favourable for the given sea states. The absorption range from the parametric sweep and GA search are 0.64 and 1.8 times the original geometry, respectively.

6. Discussion

The optimization of a floating platform for wave energy converters (WECs) involves a multi-variable problem, where the performance of the integrated wave absorbers (WAs) is influenced by various parameters. In our study, we utilized a Genetic Algorithm (GA) to explore the optimization of the geometry and dimensions of a floating platform housing pitching WECs. The objective was to improve the absorption efficiency (AEP) and range of absorption, which are critical for maximizing energy extraction from ocean waves.

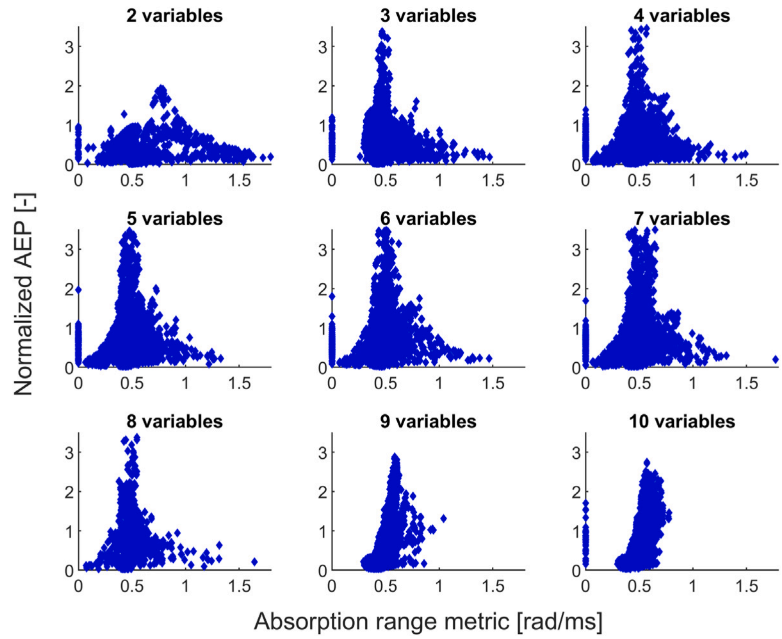

Fig. 9. The absorption range metric, W and normalized annual energy production, AEP, as in (11), for the different number of variables optimized. The variables chosen for optimization are sequentially selected; for example, 6 variables optimization contains V1, V2, V3, V4, V5 and V6.

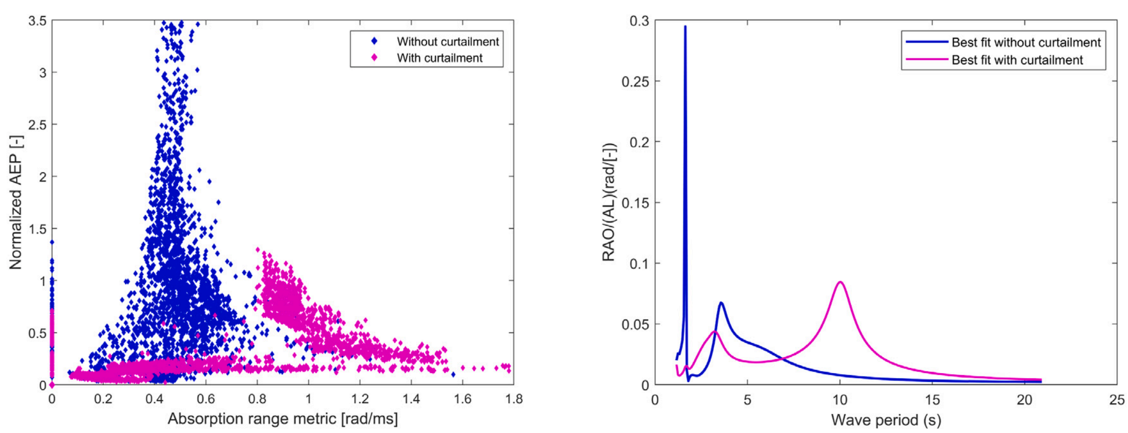

(a) (b)

Fig. 10. (a) The absorption range, W and normalized annual energy production, AEP, as in (11), for 6 variables optimized that demonstrates strong positive influence according to parametric sweep results, Fig. 6. The variables are V1, V2, V3, V4, V5 and V10 and are compared when the variables' allowed range is curtailed to remove the part that performs worse than the original geometry and when there is no curtailment. (b) The corresponding RAO for the geometries giving the best results as obtained from (a).

The choice of GA as the optimization method was based on several considerations. GA offers distinct advantages that align with the objectives of our study. Firstly, GA is known for its robustness to local optima, making it suitable for exploring complex solution spaces. This characteristic was crucial for our study, given the intricate relationships between platform geometry, wave absorber performance, and system efficiency. Secondly, GA can effectively handle non-linear relationships, which is essential for optimizing the complex 3D geometries of the floating platform. By allowing for a flexible and adaptive search process, GA enabled us to navigate the vast solution space and identify promising configurations that enhance wave energy absorption.

However, we acknowledge GA's potential limitations, including its computational intensity and sensitivity to parameter settings. Factors such as population size, generation count, and convergence criteria can influence GA's efficiency. These considerations were taken into account during the optimization process to ensure meaningful results.

The results of our optimization study revealed several important insights into the impact of different variables on the system's performance. We observed a downward trend in the number of search results achieving high AEP and absorption range as we widened the solution space to include more variables. This observation can be attributed to the low influence level of certain variables, specifically V5 to V8, as depicted in Fig. 6. These variables do not explicitly have a negative impact on fitness but, when thrown into the mix, result in an unnecessary widening of the solution space, which may have a negative impact on fitness, raising questions about their inclusion in the optimization process.

To address the issue of variables with negative impacts on fitness, it is crucial to consider their relevance in achieving the optimization objective(s). The objective of our study was to demonstrate how individual optimization variables' impact in the solution space can be identified early on, as seen in the parameter sweep results. This highlights the importance of carefully selecting and analysing variables

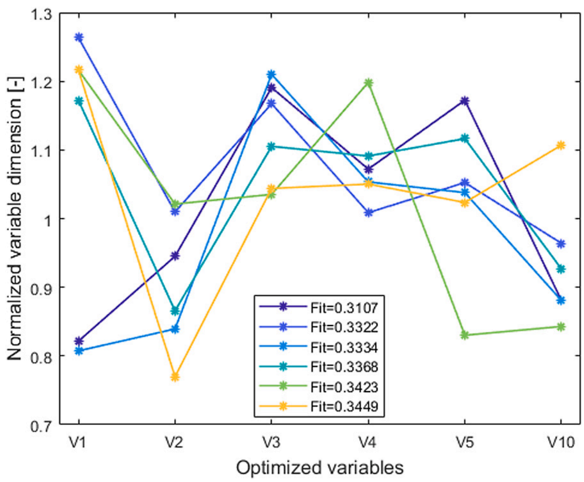

Fig. 11. Various combinations of V1, V2, V3, V4, V5, V10 variables (dimensions normalized) that result in fitness function values differing by less than 0.03.

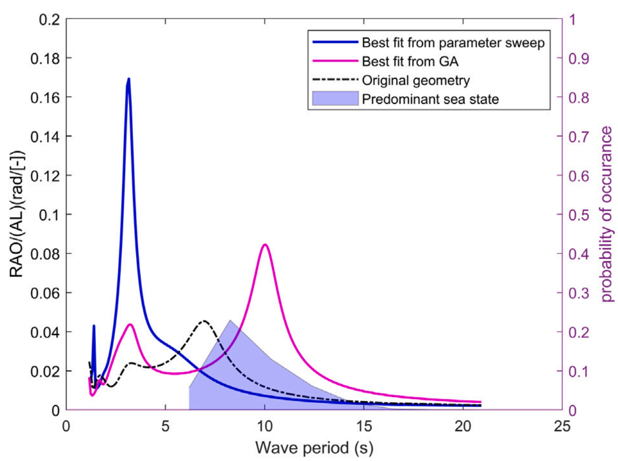

Fig. 12. Normalized response amplitude operator for the relative pitch motion of the wave absorbers for: (1) a combination of features offering best performances according to individual variables' parametric sweep, (2) considering only the most influential variables and curtailing the solution space to cancel negative influence, (3) the original geometry that we started with, and (4) peak period against the probability of occurrence.

to avoid unnecessary computational burden and to focus on those that significantly impact the desired outcomes.

One suggestion was to consider a multi-objective optimization approach, where the first fitness function (FF1) is AEP and the second fitness function (FF2) is bandwidth. While this approach could provide additional insights, it was not chosen for this study. Our focus was to optimize for AEP and absorption range simultaneously, as they are crucial for maximizing energy extraction efficiency.

Regarding the interest in wider bandwidth, our primary goal was to identify geometries where RAO maintains relatively high values within our desired bandwidth of wave periods. This consideration is vital for efficient energy extraction, as certain system geometries may exhibit spikes in RAO at specific wave periods. Our interest lies in configurations where RAO remains consistently high within the desired frequency range, ensuring optimal energy absorption across various wave conditions.

In conclusion, our study highlights the complexities involved in optimizing floating platform geometries for wave energy conversion. By utilizing GA and analysing the impact of different variables, we aimed to enhance the absorption efficiency and range of the integrated wave absorbers. The insights gained from this study contribute to the understanding of how individual optimization variables influence the system's performance and underscore the importance of careful variable selection and representation in the optimization process. Future research could explore alternative optimization methods, refine the representation of bandwidth in the objective function, and investigate additional factors impacting system performance, such as structural integrity and cost-effectiveness.

7. Conclusion

The paper contains a study using a heuristic search method to optimize the interaction between a pitching wave energy device surrounded by a floating platform. The purpose is to investigate the practicality of using the genetic algorithm to find the geometry of a platform that will interact best with the integrated WA for improved performance and explore and recommend some hacks to achieve better performance.

The study presents a GA employed for multi-variable-objective optimization. The objective, formulated as a single objective function, includes maximizing Annual Energy Production (AEP) while achieving a wide wave absorption range. The results show that in order to achieve computationally inexpensive and acceptable results for an optimization problem with several optimization parameters some of the routes to take include the following. Choose a GA search start point resulting from running a few iterations simulations in series, where the best result from one run is used as the starting point of the next one. This offered up to 6.5 times the fitness just after two runs. This is also a good way to avoid getting stuck in a local optima. Next, we observe that when there are more variables to be optimized, the number of required iterations to convergence will increase due to a broader solution space to search. This, in turn, poses a negative impact on the attained fitness value. Optimization variable curtailment is a method used in this study to narrow the solution space by identifying the variables of significant positive influence and curtailing their variation range. It shows promising results by reducing computation time by half and providing geometry that gives an overall better effect. Finally, the method shows results with a significantly better absorption range with resonance frequencies corresponding to the average peak period of the wave climate.

The methods suggested in this paper for geometry definition, and optimization can be used in other applications for submerged large structures with many characteristic features.

CRediT authorship contribution statement

Chisom Ekweoba: Conceptualization, Data curation, Formal analysis, Investigation, Methodology, Software, Validation, Writing – original draft, Writing – review & editing, Visualization. **Dan El Montoya:** Data curation, Methodology, Validation, Writing – review & editing. **Lander Galera:** Data curation, Writing – review & editing, Methodology, Validation. **Susana Costa:** Data curation, Methodology, Validation, Writing – review & editing. **Sarah Thomas:** Methodology, Resources, Software, Supervision, Writing – review & editing. **Andrej Savin:** Methodology. **Irina Temiz:** Data curation, Formal analysis, Funding acquisition, Investigation, Methodology, Project administration, Resources, Software, Supervision, Validation, Visualization, Writing – review & editing.

Declaration of competing interest

The authors declare that they have no known competing financial interests or personal relationships that could have appeared to influence the work reported in this paper.

Acknowledgements

This work was supported in part by the "OESA" project co-financed by the European Union under the European Regional Development Fund (ERDF) within the Interreg North Sea Region Programme and Swedish Energy Agency (PA No. 48347- 1), STandUP for Energy, AForsk (17-550) and Uppsala University, Sweden.

References

[1] A. Palme, Wave motion turbine, Power 52 (18) (1920) 200–201.
[2] R.W. Yeung, Y. Jiang, Shape effects on viscous damping and motion of heaving cylinders, J. Offshore Mech. Arct. Eng. 136 (4) (2014).
[3] C.A. Rodríguez, P. Rosa-Santos, F. Taveira-Pinto, Hydrodynamic optimization of the geometry of a sloped-motion wave energy converter, Ocean Eng. 199 (2020) 107046.
[4] M. Vantorre, R. Banasiak, R. Verhoeven, Modelling of hydraulic performance and wave energy extraction by a point absorber in heave, Appl. Ocean Res. 26 (1–2) (2004) 61–72.
[5] S. Jin, R.J. Patton, B. Guo, Enhancement of wave energy absorption efficiency via geometry and power take-off damping tuning, Energy 169 (2019) 819–832.
[6] L. Sjökvist, R. Krishna, M. Rahm, V. Castellucci, H. Anders, M. Leijon, On the optimization of point absorber buoys, J. Mar. Sci. Eng. 2 (2) (2014) 477–492.
[7] A. Kurniawan, T. Moan, Multi-objective optimization of a wave energy absorber geometry, in: Modelling and Geometry Optimisation of Wave Energy Converters, 2013.
[8] A. McCabe, G. Aggidis, M. Widden, Optimizing the shape of a surge-and-pitch wave energy collector using a genetic algorithm, Renew. Energy 35 (12) (2010) 2767–2775.
[9] A. McCabe, Constrained optimization of the shape of a wave energy collector by genetic algorithm, Renew. Energy 51 (2013) 274–284.
[10] Z. He, D. Ning, Y. Gou, Z. Zhou, Wave energy converter optimization based on differential evolution algorithm, Energy 246 (2022) 123433.
[11] A. Garcia-Teruel, D. Forehand, A review of geometry optimisation of wave energy converters, Renew. Sustain. Energy Rev. 139 (2021) 110593.
[12] J. Newman, Deformable floating bodies, in: 8th International Workshop on Water Waves and Floating Bodies, St. John's, Newfoundland, 1993, pp. 109–112.
[13] A. Kurniawan, D. Greaves, J. Chaplin, Wave energy devices with compressible volumes, Proc. R. Soc. Lond. Ser. A Math. Phys. Eng. Sci. 470 (2172) (2014) 20140559.
[14] S. Xu, J. Rodrigues, C.G. Soares, Hydrodynamic analysis and optimization of a wave activated device, in: Progress in Renewable Energies Offshore: Proceedings of the 2nd International Conference on Renewable Energies Offshore (RENEW2016), Lisbon, Portugal, 24-26 October 2016, CRC Press, 2016, p. 285.
[15] M. Ohsaki, Genetic algorithm for topology optimization of trusses, Comput. Struct. 57 (2) (1995) 219–225.
[16] S. Rajeev, C. Krishnamoorthy, Genetic algorithms-based methodologies for design optimization of trusses, J. Struct. Eng. 123 (3) (1997) 350–358.
[17] F. Erbatur, O. Hasançebi, İ. Tütüncü, H. Kılıç, Optimal design of planar and space structures with genetic algorithms, Comput. Struct. 75 (2) (2000) 209–224.
[18] S. Watson, A. Moro, V. Reis, C. Baniotopoulos, S. Barth, G. Bartoli, F. Bauer, E. Boelman, D. Bosse, A. Cherubini, et al., Future emerging technologies in the wind power sector: A European perspective, Renew. Sustain. Energy Rev. 113 (2019) 109270.
[19] K. Hasselmann, T.P. Barnett, E. Bouws, H. Carlson, D.E. Cartwright, K. Enke, J. Ewing, A. Gienapp, D. Hasselmann, P. Kruseman, et al., Measurements of wind-wave growth and swell decay during the joint north sea wave project (JONSWAP), Ergaenzungsheft Dtsch. Hydrogr. Z. Reihe A (1973).
[20] A.M. Cornett, A global wave energy resource assessment, in: The Eighteenth International Offshore and Polar Engineering Conference, OnePetro, 2008.
[21] S. Ahn, Modeling mean relation between peak period and energy period of ocean surface wave systems, Ocean Eng. 228 (2021) 108937, http://dx.doi.org/10.1016/j.oceaneng.2021.108937, URL https://www.sciencedirect.com/science/article/pii/S0029801821003723.
[22] WAMIT, User manual version 7.0, 2013, p. 350, URL http://www.wamit.com/manual.htm.
[23] P. Heras, S. Thomas, M. Kramer, J.P. Kofoed, Numerical and experimental modelling of a wave energy converter pitching in close proximity to a fixed structure, J. Mar. Sci. Eng. 7 (7) (2019) 218.
[24] I. Temiz, C. Ekweoba, S. Thomas, M. Kramer, A. Savin, Wave absorber ballast optimization based on the analytical model for a pitching wave energy converter, Ocean Eng. 240 (2021) 109906.
[25] S. Thomas, S. Thor, 800-FPP-0011 parametric study of platform dimensions working draft, 2022, unpublished.
[26] R.L. Haupt, S.E. Haupt, Practical Genetic Algorithms, John Wiley & Sons, 2004.
[27] O. Faltinsen, Sea Loads on Ships and Offshore Structures, Vol. 1, Cambridge University Press, 1993.